

Enthalpy – based homogenization procedure for composite piezoelectric modules with integrated electrodes

Burkhard Kranz^{*1}, Ayech Benjeddou² and Welf-Guntram Drossel³

¹Fraunhofer Institute for Machine Tools and Forming Technology, 01187 Dresden, Germany

²Institut Supérieur de Mécanique de Paris, 93400 Saint-Ouen, France

³Institute for Machine Tools and Production Processes, Chemnitz University of Technology, 09107 Chemnitz, Germany

(Received February 15, 2013, Revised June 14, 2013, Accepted August 10, 2013)

Abstract. A new enthalpy – based procedure for the homogenization of the electromechanical material parameters of composite piezoelectric modules with integrated electrodes is presented. It is based on a finite element (FE) modeling of the latter's representative volume element (RVE). In contrast to most previously published homogenization approaches that are based on averaged quantities, the presented method uses a direct evaluation of the electromechanical enthalpy. Hence, for the linear orthotropic piezoelectric composite behavior full set of elastic, piezoelectric, and dielectric material parameters, 17 load cases (LC) are used where each load case leads directly to one material parameter. This gives the possibility to elaborate a very strict and easy to program processing. In conjunction with the 17 LC, the enthalpy – based homogenization is particularly suitable for laminated composite piezoelectric modules with integrated electrodes. In this case, the electric load has to be given at the electrodes rather than at the RVE FE model boundaries. The proposed procedure is validated through its comparison to literature available results on a classical 1-3 piezoelectric micro fiber (longitudinally polarized) reinforced composite and a d_{15} shear piezoelectric macro-fiber (transversely polarized) composite module.

Keywords: electromechanical enthalpy; finite element homogenization; piezoelectric composite modules; integrated electrodes

1. Introduction

Piezoelectric modules, as sensors, actuators or transducers for structural noise, shape, vibration, and health control, often use thin piezoceramic elements like plates, rods, or fibers and suitable electrodes to measure (for sensor functionality) or provide (for actuator functionality) the electric field. The focus on thin piezoceramic structures allows the limitation of the driving voltage to provide the necessary electric field strength. The packaging of these piezoelectric modules involves also mainly metallic electrodes, epoxy resin and protection layers beside the piezoceramic host structures (see Fig. 1).

To numerically incorporate such piezoelectric modules with thin piezoceramic host structures (dimension in the order of 100 μm) into simulation models of the according structural part or

*Corresponding author, Research Associate, E-mail: burkhard.kranz@iwu.fraunhofer.de

overall system (dimension in the order of meters) homogenized material parameters have to be used. A detailed discretization and simulation of the overall model, based on the geometry of the packaging and in the order of magnitude of the thin piezoceramic host structures, can be done but requires high-performance computing technology (parallel multi-frontal solver), see for example (Paik *et al.* 2007). Besides, in order to obtain the effective material properties, namely elastic, piezoelectric, and dielectric constants, of such piezoelectric modules, not only the epoxy-to-piezoceramic fiber volume fraction (FVF) has to be considered but also the influence of the inner electrodes and the protection layers.

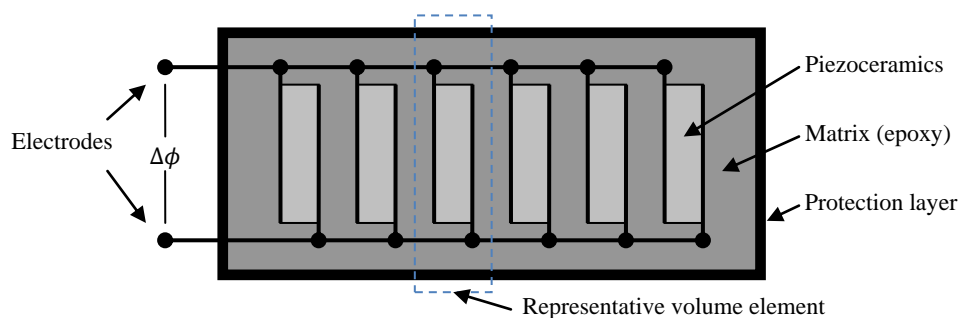


Fig. 1 Schematic of a piezoelectric module with integrated electrodes and protective layers (not to scale)

Various homogenization methods have been applied to determine the effective material properties of composite piezoelectric modules. The use of analytical methods from the composite materials literature (Pindera *et al.* 2009), such as the Asymptotic Homogenization Method (AHM) and the Uniform Field Method (UFM) (see for e.g., Benjeddou and Al-Ajmi 2011, Biscani *et al.* 2011, Deraemaeker *et al.* 2009), is normally limited to the active layer of the laminated composite piezoelectric transducers. The use of techniques based on finite element (FE) models (see for e.g., Trindade and Benjeddou 2011, Shindo *et al.* 2011) gives a broader freedom to study different topologies and geometries and provide the possibility to incorporate electrodes and protective layers in the homogenization model. For periodically constructed composites the determination of effective material parameters is generally based on a FE model of a representative volume element (RVE). It's important to mention that for the consideration of whole piezoelectric modules the electrodes should be included in the RVE.

In the present work a FE homogenization method is introduced which uses a direct evaluation of the RVE electromechanical enthalpy that handles well the electrodes inside the composite piezoelectric modules. In this case, and in compliance with the real electric field distribution, the electric load has to be given at the electrodes and not at the FE model boundaries as is often done in the open literature. Otherwise, this conflicts with the assumption of homogeneous boundary conditions of the RVE when using averaged quantities for stresses, strains, dielectric displacements and electric fields as in other classical FE homogenization methods. An alternative way for dealing with electrodes inside the relevant RVE was given in (Deraemaeker *et al.* 2010) by introducing macro variables for the electric quantities at the electrodes. Therefore, in (Deraemaeker *et al.* 2010) the processing differs for the mechanical and the electrical parts of the

FE model. In the here presented work mechanical and electrical parts can be handled in the same way.

It's worthy to notice that for the elastic constants evaluation the proposed Enthalpy – based Homogenization Method (EBHM) is the same as the so-called Strain – based Homogenization Method (SBHM), see for example (Xu *et al.* 2010, Zhang *et al.* 2007). Hence, the former approach can be seen as an extension of the latter, devoted to elastic composites, to piezoelectric composites.

Recently, the SBHM combined to a Dielectric Energy – based Homogenization Method (DEHM) has been used for the evaluation of the elastic and dielectric constants, respectively, of multi-phase piezoelectric composites (Malakooti and Sodano 2013). However, average strain-to-electric field ratios have been used to compute the strain piezoelectric constants. Hence, this is a combined use of SBHM, EBHM and the classical Average Quantity – based Homogenization Method (AQBH). It can be then concluded that the presently proposed EBHM is the only approach that handles all electromechanical (elastic, piezoelectric and dielectric) constants similarly; this is the main originality of this contribution, together with the correct modeling of piezoelectric RVE integrating inner electrodes.

Hereafter, the basic idea of the FE homogenization and the classical AQBH are first presented, followed by this proposed new EBHM. The latter is then validated by its application to a 1-3 longitudinally poled piezoelectric fiber composite and its comparison to the AQBH by (Berger *et al.* 2006) and (Pettermann and Suresh 2000). Next, the EBHM is demonstrated on a hypothetically transversely polarized shear Macro-Fiber Composite (MFC) concept and corresponding AQBH by (Trindade and Benjeddou 2011). Finally, conclusions and perspectives are provided as a closure.

2. Finite element homogenization of piezoelectric composites

2.1 Basic idea of FE homogenization

The main idea for the evaluation of the effective properties of composites is the energetic equality of a chosen composite volume and a corresponding homogeneous material volume under the same boundary conditions. For periodic composites the considerations can be based on a RVE of the composite or rather a detailed FE model of the RVE. So, it is required that

$$W_{\text{RVE, FE}} = W_{\text{RVE, homogeneous}} \quad (1)$$

Where, $W_{\text{RVE, FE}}$ gives the energy content of the detailed RVE FE model, and $W_{\text{RVE, homogeneous}}$ stands for the energy of the homogeneous material with an equal volume as the RVE.

For piezoelectric modules for which we want to describe the functional behavior at a working point, the linear elastic, piezoelectric and dielectric material parameters have to be considered. Due to the *packaging* and the influence of the *protection layers* the behavior of the composite piezoelectric modules has to be considered as *orthotropic* even though the typically used polycrystalline piezoceramic materials behave as transverse isotropic. Hence, using the Voigt notation, the three-dimensional (3D) linear piezoelectric constitutive equations, written in a condensed *e-form*, are

$$\begin{pmatrix} \bar{T}_1 \\ \bar{T}_2 \\ \bar{T}_3 \\ \bar{T}_4 \\ \bar{T}_5 \\ \bar{T}_6 \\ \bar{D}_1 \\ \bar{D}_2 \\ \bar{D}_3 \end{pmatrix} = \begin{pmatrix} \bar{c}_{11}^E & \bar{c}_{12}^E & \bar{c}_{13}^E & 0 & 0 & 0 & 0 & 0 & -\bar{e}_{31} \\ \bar{c}_{12}^E & \bar{c}_{22}^E & \bar{c}_{23}^E & 0 & 0 & 0 & 0 & 0 & -\bar{e}_{32} \\ \bar{c}_{13}^E & \bar{c}_{23}^E & \bar{c}_{33}^E & 0 & 0 & 0 & 0 & 0 & -\bar{e}_{33} \\ 0 & 0 & 0 & \bar{c}_{44}^E & 0 & 0 & 0 & -\bar{e}_{24} & 0 \\ 0 & 0 & 0 & 0 & \bar{c}_{55}^E & 0 & -\bar{e}_{15} & 0 & 0 \\ 0 & 0 & 0 & 0 & 0 & \bar{c}_{66}^E & 0 & 0 & 0 \\ 0 & 0 & 0 & 0 & \bar{e}_{15} & 0 & \bar{\epsilon}_{11}^S & 0 & 0 \\ 0 & 0 & 0 & \bar{e}_{24} & 0 & 0 & 0 & \bar{\epsilon}_{22}^S & 0 \\ \bar{e}_{31} & \bar{e}_{32} & \bar{e}_{33} & 0 & 0 & 0 & 0 & 0 & \bar{\epsilon}_{33}^S \end{pmatrix} \cdot \begin{pmatrix} \bar{S}_1 \\ \bar{S}_2 \\ \bar{S}_3 \\ \bar{S}_4 \\ \bar{S}_5 \\ \bar{S}_6 \\ \bar{E}_1 \\ \bar{E}_2 \\ \bar{E}_3 \end{pmatrix} \quad (2)$$

Where, \bar{T}_p , \bar{S}_q , \bar{D}_i , and \bar{E}_j ($p, q = 1, \dots, 6$; $i, j = 1, \dots, 3$) are, respectively, the components of the effective stress, strain, electric displacement and field vectors, and \bar{c}_{pq}^E , \bar{e}_{jp} , and $\bar{\epsilon}_{ij}^S$ are those of the effective elastic (at constant electric field – *shorted*), stress piezoelectric and dielectric (at constant strain – *blocked*) matrices. The over bar indicates that the quantities are interpreted as effective quantities describing the behavior of the piezoelectric module in a homogeneous way. In Eq. (2), the 3-direction gives the direction of polarization of the piezoceramic material.

Choosing the electromechanical enthalpy density

$$H = \frac{1}{2} (T_p S_p - D_i E_i) \quad (3)$$

as thermodynamic potential of the piezoelectric problem we request, from Eq. (1), that Eq. (2) observes

$$\frac{1}{2 V_{\text{RVE}}} \int_{V_{\text{RVE}}} (T_p S_p - D_i E_i) dV = \frac{1}{2} (\bar{T}_p \bar{S}_p - \bar{D}_i \bar{E}_i) \quad (4)$$

Using Eq. (2), the right hand side of Eq. (4) can be written as

$$\frac{1}{2} (\bar{T}_p \bar{S}_p - \bar{D}_i \bar{E}_i) = \frac{1}{2} \bar{S}_p \bar{c}_{pq}^E \bar{S}_q - \bar{E}_i \bar{e}_{ip} \bar{S}_p - \frac{1}{2} \bar{E}_j \bar{\epsilon}_{ji}^S \bar{E}_i \quad (5)$$

2.2 Averaged quantities – based homogenization method (AQBH)

To evaluate the effective material parameters \bar{c}_{pq}^E , \bar{e}_{jp} , and $\bar{\epsilon}_{ij}^S$ the standard way is to determine effective (*averaged*) stress \bar{T}_p , strain \bar{S}_q , electric displacement \bar{D}_i , and electric field \bar{E}_j from the FE model of the RVE and to exploit Eq. (5) (Trindade and Benjeddou 2011); these averaged quantities are defined by

$$\bar{A} = \frac{1}{V_{\text{RVE}}} \int_{V_{\text{RVE}}} A dV \quad \text{with } A = \{T_p, S_q, D_i, E_j\} \quad (6)$$

They are approximated from the FE Model by

$$\bar{A} = \frac{\sum_{n=1}^N A^{(n)} V^{(n)}}{\sum_{n=1}^N V^{(n)}} \quad (7)$$

With, N , $A^{(n)}$, and $V^{(n)}$ being the number of finite elements, quantity, and volume at n^{th} FE of the RVE model.

To achieve energetic equivalence according to Eqs. (1) and (4) with this procedure, special boundary conditions have to be chosen on the RVE boundary Γ_{RVE} . In (Hori and Nemat-Nasser 1998) and (He 2004) the Hill–Mandel–condition (macro-homogeneity condition) is extended to piezoelectric materials; it is shown that Eq. (4) holds if and only if

$$\int_{\Gamma_{\text{RVE}}} [(u_i - \bar{\varepsilon}_{ij} x_j)(\sigma_{ij} n_j - \bar{\sigma}_{ij} n_j) - (\phi + \bar{E}_j x_j)(D_j n_j - \bar{D}_j n_j)] d\Gamma = 0 \quad (8)$$

Where, u_i , x_j , n_j , and ϕ are, respectively, the components of the mechanical displacement and position vectors, of the outward normal unit vector at the boundary, and the electric potential. Here, for convenience, stress and strain tensor components were denoted as σ_{ij} and ε_{ij} , respectively.

One possibility to fulfill Eq. (8) is to choose *homogeneous* boundary conditions for the RVE FE model according to the displacement components and the electric potential so that

$$u_i = \bar{\varepsilon}_{ij} x_j \quad \text{and} \quad \phi = -\bar{E}_j x_j \quad \text{on } \Gamma_{\text{RVE}} \quad (9)$$

In relation to composite piezoelectric modules with *integrated* electrodes and protective layers, the electric potential input at the boundaries of the RVE does not reflect the real electric field distribution; this is because the actual electric field follows the electric excitation at the electrodes but not at the RVE boundaries (see Fig. 1).

2.3 Enthalpy – based homogenization method (EBHM)

To overcome the aforementioned conflict for the electric boundary conditions we propose a new evaluation scheme to ensure energetic equivalence according to Eqs. (1) and (4). The left hand side of Eq. (4) can be evaluated element-wise and summed over the whole FE model afterwards so that we can approximate the RVE electromechanical enthalpy density from its FE model directly as

$$2 \cdot H_{\text{RVE,FE}} = \frac{\sum_{n=1}^N (T_p^{(n)} S_p^{(n)} - D_i^{(n)} E_i^{(n)}) \cdot V^{(n)}}{\sum_{n=1}^N V^{(n)}} \quad (10)$$

The application of the constitutive Eq. (2) to the right hand side of Eq. (4) leads to this expression (in Voigt notation)

$$\begin{aligned} 2 \cdot H_{\text{RVE,homogen}} = & \bar{c}_{11}^E \bar{S}_1^2 + \bar{c}_{22}^E \bar{S}_2^2 + \bar{c}_{33}^E \bar{S}_3^2 + \bar{c}_{44}^E \bar{S}_4^2 + \bar{c}_{55}^E \bar{S}_5^2 + \bar{c}_{66}^E \bar{S}_6^2 + 2\bar{c}_{12}^E \bar{S}_1 \bar{S}_2 \\ & + 2\bar{c}_{13}^E \bar{S}_1 \bar{S}_3 + 2\bar{c}_{23}^E \bar{S}_2 \bar{S}_3 - 2\bar{e}_{31}^E \bar{E}_3 \bar{S}_1 - 2\bar{e}_{32}^E \bar{E}_3 \bar{S}_2 - 2\bar{e}_{33}^E \bar{E}_3 \bar{S}_3 - 2\bar{e}_{24}^E \bar{E}_2 \bar{S}_4 \\ & - 2\bar{e}_{15}^E \bar{E}_1 \bar{S}_5 - 2\bar{\varepsilon}_{11}^S \bar{E}_1^2 - 2\bar{\varepsilon}_{22}^S \bar{E}_2^2 - 2\bar{\varepsilon}_{33}^S \bar{E}_3^2 \end{aligned} \quad (11)$$

We can see that it is easy to construct load cases of the RVE depending on \bar{S}_q and \bar{E}_j in such a way that only one unknown effective material parameter is active one after another. For all 17 material parameters of the piezoelectric constitutive Eq. (2) we construct 17 load cases (LC). When we use unit loads $\bar{S}_q = 1$ and $\bar{E}_j = 1$ the enthalpy density $H_{\text{RVE,FE}}$ of the FE model of the RVE gives the active material parameter directly as shown in Table 1.

Table 1 Complete set of load cases for EBHM of linear piezoelectric composites

Load case	\bar{S}_1	\bar{S}_2	\bar{S}_3	\bar{S}_4	\bar{S}_5	\bar{S}_6	\bar{E}_1	\bar{E}_2	\bar{E}_3	Resulting material parameter
LC01	1	0	0	0	0	0	0	0	0	$\bar{c}_{11}^E = 2 H_{\text{RVE,FE,LC01}}$
LC02	0	1	0	0	0	0	0	0	0	$\bar{c}_{22}^E = 2 H_{\text{RVE,FE,LC02}}$
LC03	0	0	1	0	0	0	0	0	0	$\bar{c}_{33}^E = 2 H_{\text{RVE,FE,LC03}}$
LC04	0	0	0	1	0	0	0	0	0	$\bar{c}_{44}^E = 2 H_{\text{RVE,FE,LC04}}$
LC05	0	0	0	0	1	0	0	0	0	$\bar{c}_{55}^E = 2 H_{\text{RVE,FE,LC05}}$
LC06	0	0	0	0	0	1	0	0	0	$\bar{c}_{66}^E = 2 H_{\text{RVE,FE,LC06}}$
LC07	1	1	0	0	0	0	0	0	0	$\bar{c}_{12}^E = (2 H_{\text{RVE,FE,LC07}} - \bar{c}_{11}^E - \bar{c}_{22}^E)/2$
LC08	1	0	1	0	0	0	0	0	0	$\bar{c}_{13}^E = (2 H_{\text{RVE,FE,LC08}} - \bar{c}_{11}^E - \bar{c}_{33}^E)/2$
LC09	0	1	1	0	0	0	0	0	0	$\bar{c}_{23}^E = (2 H_{\text{RVE,FE,LC09}} - \bar{c}_{22}^E - \bar{c}_{33}^E)/2$
LC10	0	0	0	0	0	0	1	0	0	$\bar{\epsilon}_{11}^S = 2 H_{\text{RVE,FE,LC10}}$
LC11	0	0	0	0	0	0	0	1	0	$\bar{\epsilon}_{22}^S = 2 H_{\text{RVE,FE,LC11}}$
LC12	0	0	0	0	0	0	0	0	1	$\bar{\epsilon}_{33}^S = 2 H_{\text{RVE,FE,LC12}}$
LC13	0	0	1	0	0	0	0	0	1	$\bar{e}_{33} = (2 H_{\text{RVE,FE,LC13}} - \bar{c}_{33}^E - \bar{\epsilon}_{33}^S)/2$
LC14	1	0	0	0	0	0	0	0	1	$\bar{e}_{31} = (2 H_{\text{RVE,FE,LC14}} - \bar{c}_{11}^E - \bar{\epsilon}_{33}^S)/2$
LC15	0	1	0	0	0	0	0	0	1	$\bar{e}_{32} = (2 H_{\text{RVE,FE,LC15}} - \bar{c}_{22}^E - \bar{\epsilon}_{33}^S)/2$
LC16	0	0	0	1	0	0	0	1	0	$\bar{e}_{24} = (2 H_{\text{RVE,FE,LC16}} - \bar{c}_{44}^E - \bar{\epsilon}_{22}^S)/2$
LC17	0	0	0	0	1	0	1	0	0	$\bar{e}_{15} = (2 H_{\text{RVE,FE,LC17}} - \bar{c}_{55}^E - \bar{\epsilon}_{11}^S)/2$

It is worthy to emphasize that this evaluation scheme is applicable for all piezoelectric composites for which the constitutive Eq. (2) is valid. In practice, a scale factor for the effective electric field quantities is involved to minimize the numerical error due to calculating the difference of quantities of different magnitudes. The main advantage in comparison to evaluation schemes with a reduced number of load cases, such as in (Trindade and Benjeddou 2011), is the very strict and easy to program processing. The disadvantage concerning the cost of calculating all 17 load cases is low considering nowadays powerful computers. The load cases are static load cases without nonlinearities. It's worthy to notice also that the combined load cases LC07 to LC09 and LC13 to LC17 are in fact superpositions of the basic load cases LC01 to LC06 and LC10 to LC12. Nevertheless, the electromechanical enthalpy for the combined load cases has to be determined based on the superposed field distributions.

To validate this new evaluation scheme we use a FE model of a transverse isotropic, piezoelectric composite with 60% FVF as given in (Berger *et al.* 2006, Pettermann and Suresh 2000) and shown in Fig. 2. This example does not consider a whole piezoelectric module with inner electrodes; so, the RVE incorporates only a piezoelectric fiber and epoxy filler. Effective material parameters obtained using the AQBH and the new EBHM scheme should be coincident.

In Table 2 we give a comparison of the results from (Berger *et al.* 2006, Pettermann and Suresh 2000) obtained with the AQBH and our results, obtained with EBHM. For comparability, the effective material parameters \bar{c}_{pq}^E , \bar{e}_{jp} , and $\bar{\epsilon}_{ij}^S$ as calculated according to Table 1 were converted to \bar{c}_{pq}^D (effective mechanical stiffness at constant electric displacement), \bar{h}_{jp} (effective piezoelectric h -constants), and $\bar{\beta}_{ij}^S$ (effective reciprocal permittivity at constant strain) according to the h -form of piezoelectric constitutive equations ($T_p = c_{pq}^D S_q - h_{jp} D_j$; $E_i = -h_{iq} S_q + \beta_{ij}^S D_j$).

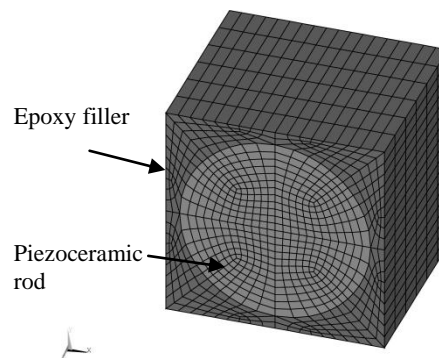


Fig. 2 RVE FE model of a piezoceramic composite with 60% FVF of cylindrical piezoelectric fibers without consideration of electrodes

Table 2 Comparison of linear piezoelectric effective material parameters for piezoceramic composite with 60% FVF without consideration of electrodes

Constants	\bar{c}_{11}^D	\bar{c}_{12}^D	\bar{c}_{13}^D	\bar{c}_{33}^D	\bar{c}_{44}^D	\bar{c}_{66}^D	\bar{h}_{31}	\bar{h}_{33}	\bar{h}_{15}	$\bar{\beta}_{11}^S$	$\bar{\beta}_{33}^S$
Unit	GPa						GV/m			GVm/C	
EBHM (Present)	25.06	8.79	10.81	87.10	6.67	4.61	-0.157	5.035	0.328	6.372	0.780
AQBH (Berger <i>et al.</i> 2006)	25.17	8.71	10.82	86.97	6.66	4.64	-0.157	5.034	0.328	6.364	0.781
AQBH (Pettermann and Suresh 2000)	25.19	8.76	10,84	87.10	6.70	4.64	-0.157	5.034	0.330	6.341	0.780

As expected the differences between the effective material parameters obtained with the different evaluation schemes are minimal. We can conclude that for piezoelectric composites *without* inner electrodes the new evaluation method EBHM complies with the classical AQBH.

2.4 Composite modules with integrated electrodes

The main purpose of effective material parameters is to use these parameters in homogeneous FE models. To reduce calculation costs these FE models should be based on FE meshes which are

coarser than the real geometric design of the piezoelectric modules would require when using inhomogeneous, detailed FE models.

Hence, starting from very detailed FE models of the composite piezoelectric modules two mesh criteria exist:

- The dimensions of the piezoceramic host structures and packaging constituents on the one hand and,
- The location (and *distance*) of the electrodes on the other hand.

From a practical point of view these two points are very closely connected because the dimensions of the piezoceramic host structures define the electrodes distance. From a simulation point of view these two points address two different aspects:

- The dimensions of the constituents describe the material inhomogeneity and,
- The locations of the electrodes give the places of the electrical boundary conditions, mainly potential input and therefore starting and end of electric field lines.

The influence of the material inhomogeneity on the mesh density can be suspended by effective material parameters. Otherwise, without dissolving the aspect of the location of the electrical boundary conditions, the mesh density cannot be efficiently reduced because electrodes distance and dimensions of constituents are in the same order of magnitude. Hence, to gain a sufficiently coarse mesh the electrical load on the piezoelectric modules has also to be homogenized. Fig. 3 illustrates this homogenization task.

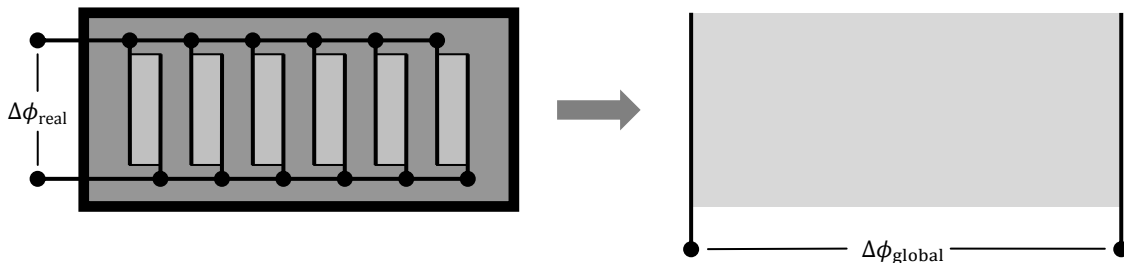


Fig. 3 Schematic of electric load homogenization

Homogenization of the electrical load means that the electric field distribution of the homogeneous RVE does not coincide with the real electric field distribution of the inhomogeneous RVE in detail. To use a global electric load as shown in Fig. 3, the electric load at the homogeneous RVE has to be given at the boundary of the homogeneous RVE. The real electric field distribution of the inhomogeneous RVE is governed by the electric load at the inner electrodes. Nevertheless, the basic idea of homogenization, namely energetic equivalence of inhomogeneous and homogeneous RVE, persists. To discuss this further, let's give a look at the dielectric energy density H_{elec} (as part of the electromechanical enthalpy density) of a one-dimensional (1D) potential driven electric field with $E = -\Delta\phi/b$, whereby b denotes the electrodes distance

$$H_{\text{elec}} = \frac{1}{2} \epsilon^S \frac{(\Delta\phi)^2}{b^2} \quad (12)$$

From Eq. (12) we can see, if the relevant electrodes distance b (or length of field lines) changes with the transition from inhomogeneous to homogeneous RVE ($b_{\text{real}} \rightarrow b_{\text{homogen}}$) we have two possibilities to ensure equivalence of the energy density, H_{elec} : we can adjust the permittivity ϵ^S and/or the electric load $\Delta\phi$. Clearly, the effective permittivity $\bar{\epsilon}^S$ is dependent on the chosen electric load $\Delta\phi_{\text{homogen}}$ for the homogeneous RVE. This discussion also holds in concern of the piezoelectric energy density (with linear dependence of the energy density on $1/b$) and leads to the same conclusion concerning the effective piezoelectric stress constant \bar{e} .

Summing up, the electric relevant effective material parameters $\bar{\epsilon}^S$ and \bar{e} depend on the arbitrarily chosen electric load on the homogeneous RVE. With other words, the specification of effective material parameters for piezoelectric modules with integrated electrodes is only consistent in connection with the specification of the homogenized electric load.

A reasonable and already used (Deraemaeker and Nasser 2010) postulate for this is the application of the real potential difference at the electrodes $\Delta\phi_{\text{real}}$ also as electric load at the boundaries of the homogeneous RVE ($\Delta\phi_{\text{RVE}}$). This postulate leads to a global electric load $\Delta\phi_{\text{global}}$ as n -fold of the real potential difference $\Delta\phi_{\text{real}}$ for driving the piezoelectric module as shown in Fig. 4. This postulate will be used in section 3. It is worth to highlight that this postulate may be obvious, but any other selection would do it also, provided that the effective material parameters conform to it. For instance, another convenient approach is to use the real potential difference $\Delta\phi_{\text{real}}$ as global potential difference $\Delta\phi_{\text{global}}$ of the homogenized simulation model. This leads to $\Delta\phi_{\text{RVE}} = \Delta\phi_{\text{real}}/n$.

From above discussion we have to conclude, that the effective material parameters cannot really be called *material* parameters when dealing with whole piezoelectric modules including inner electrodes. This is because the effective parameters describing the electromechanical behavior of the module depend not only on the constituent materials but also on the reference electric load.

Keeping this in mind, we stick to the previously used term *effective material parameters*, because in the global simulation model they will be inputted as such material parameters.

3. Application to shear piezoelectric macro-fiber composites

3.1 RVE FE model and associated boundary conditions

Now, we want to demonstrate the implementation of the boundary conditions for the load cases of Table 1 on an example previously published in (Trindade and Benjeddou 2011). In the latter, the effective material parameters were estimated based on averaged stresses, strains, electric displacements, and electric fields. The material parameters were obtained with 7 load cases which correspond partly (for the 6 mechanical load cases) to our load cases LC01 to LC06. However, the electrical load case (LC07) used in (Trindade and Benjeddou 2011) does not have any displacement constraints and does not correspond to any of the load cases in Table 1.

We look hereafter at a shear piezoelectric macro-fiber composite which layup is as in Fig. 5.

A detailed description of the shear piezoelectric MFC is given in (Trindade and Benjeddou 2011) including dimensions and used material properties. We present here the FE model and results for the design with 86% FVF relating to the active layer. Due to a difference of electric potential between the electrode layers an electric field (x_1 -direction) perpendicular to the polarization direction of the piezoceramic rods or fibers (x_3 -direction) is impressed. This leads to a shear deformation in the x_1 - x_3 plane, thus S_5 (respectively, \bar{S}_5). With this electrode configuration the electric field is applicable only in x_1 -direction. Therefore we concentrate on those load cases of Table 1, which incorporate $\bar{E}_1 = 1$.

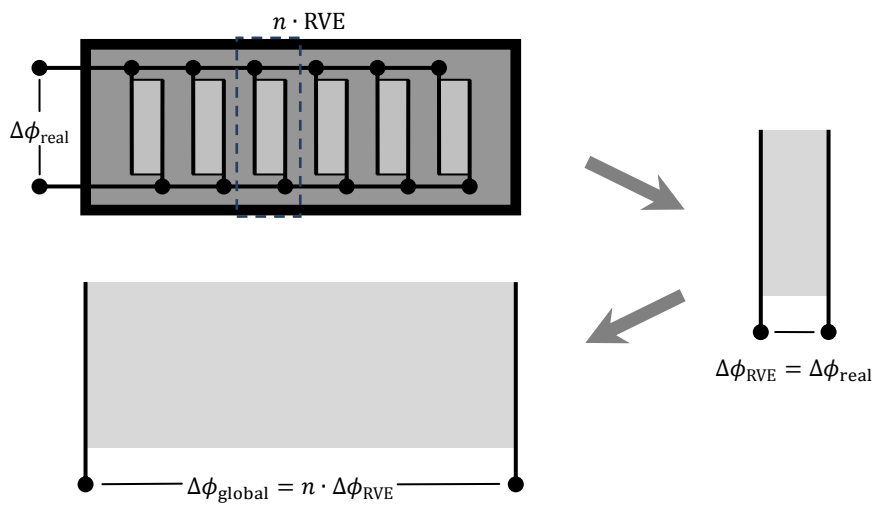


Fig. 4 Electric load on RVE and global model

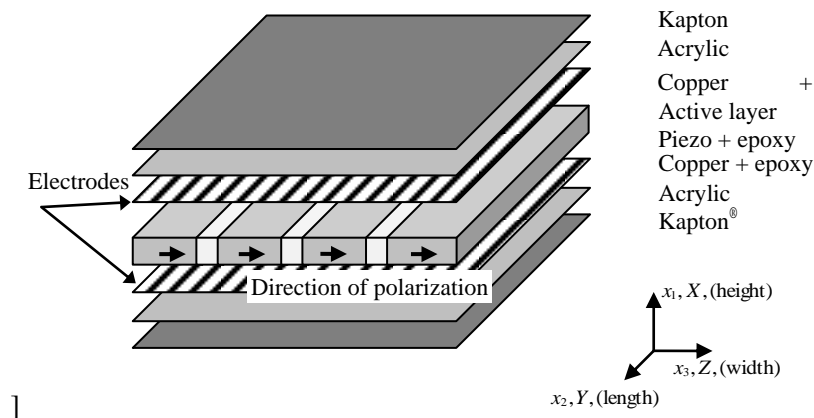


Fig. 5 Schematic exploded view of a transversely polarized shear piezoelectric MFC as in (Trindade and Benjeddou 2011)

Using ANSYS® for the FE simulations, the shear MFC RVE FE model, as shown in Fig. 6, is composed of 5525 SOLID226 (quadratic, coupled field) elements with 20 nodes and 4 degrees of freedom (DOF) per node: 3 translations u_i and 1 electric potential ϕ ; the mesh is created by 13 divisions along the Y -axis, 17 divisions along the Z -axis (11 divisions for the length of the piezoceramic fiber, 3 divisions for each epoxy region), and 25 divisions (2 divisions for each of the six top- and bottom-layers and 13 divisions in the height of the active layer) along the X -axis.

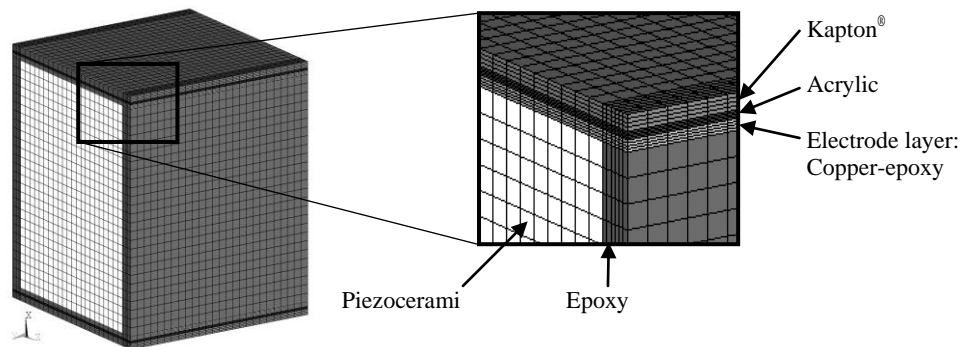


Fig. 6 FE model of the RVE of the shear piezoelectric MFC

The electric potential DOF of all nodes of each electrode layer respectively (X^{El-}/X^{El+}) is coupled in order to fulfill the physical equipotential conditions of the electrodes. Therefore, a direct electrical potential connection (short circuit) between the model boundaries Y^-/Y^+ and Z^-/Z^+ exists. This implies that load cases with an effective electric field in Y -direction ($\bar{E}_2 = 1$) and Z -direction ($\bar{E}_3 = 1$) are not possible from the modeling point of view. So the aforementioned concentration of the load cases with $\bar{E}_1 = 1$ is sufficient to represent the electrical behavior of the MFC piezoelectric module. Anyhow, the numbering of the load cases still follows Table 1. So we consider the relevant load cases LC01 to LC10 and LC17 to the shear actuation mechanism.

The actual boundary conditions for the load cases have to ensure periodicity of the model and impress effective strain and/or effective electric field according to Table 1. This can be achieved by using constraint equations between the DOF of corresponding nodes belonging to two opposite faces of the studied RVE. In other words, a relation is applied to all DOF of all pairs of nodes located on both of the indicated faces. These constraint equations are directly derived from Eq. (9).

Table 3 gives an overview of all used constraint equations with the following related remarks:

- In the head of the table the left hand sides of the constraint equations are given.
- The right hand sides (or inhomogeneous parts) of the constraint equations are given in the body of the table assigned to the load cases.
- The subscripts refer to the displacement's direction.
- The + or – in the superscript indicates the superior or the inferior face.
- The El superscript indicates that the potential is applied to the electrodes of the FE model.
- The potential relations $\phi^{Y^+} - \phi^{Y^-} = 0$ and $\phi^{Z^+} - \phi^{Z^-} = 0$ ensure the periodicity of the potential on the lateral faces of the RVE.
- ΔX_{RVE} , ΔY_{RVE} , and ΔZ_{RVE} are the dimensions of the RVE in the particular direction. The

use of these terms as the inhomogeneous parts of the constraint equations leads to unit loads of effective strains and effective electric fields.

Table 3 EBHM constraint equations of load cases for the homogenization of the shear MFC

Load case	\bar{S}_1	\bar{S}_2	\bar{S}_3	\bar{S}_4	\bar{S}_5	\bar{S}_6	\bar{E}_1	\bar{E}_2	\bar{E}_3
	$u_1^{X+} - u_1^{X-}$	$u_2^{Y+} - u_2^{Y-}$	$u_3^{Z+} - u_3^{Z-}$	$u_2^{Z+} - u_2^{Z-}$ $u_3^{Y+} - u_3^{Y-}$	$u_1^{Z+} - u_1^{Z-}$ $u_3^{X+} - u_3^{X-}$	$u_1^{Y+} - u_1^{Y-}$ $u_2^{X+} - u_2^{X-}$	$\phi^{El+} - \phi^{El-}$	$\phi^{Y+} - \phi^{Y-}$	$\phi^{Z+} - \phi^{Z-}$
LC01	ΔX_{RVE}	0	0	0	0	0	0	0	0
LC02	0	ΔY_{RVE}	0	0	0	0	0	0	0
LC03	0	0	ΔZ_{RVE}	0	0	0	0	0	0
LC04	0	0	0	$\Delta Z_{RVE}/2$ $\Delta Y_{RVE}/2$	0	0	0	0	0
LC05	0	0	0	0	$\Delta Z_{RVE}/2$ $\Delta X_{RVE}/2$	0	0	0	0
LC06	0	0	0	0	0	$\Delta Y_{RVE}/2$ $\Delta X_{RVE}/2$	0	0	0
LC07	ΔX_{RVE}	ΔY_{RVE}	0	0	0	0	0	0	0
LC08	ΔX_{RVE}	0	ΔZ_{RVE}	0	0	0	0	0	0
LC09	0	ΔY_{RVE}	ΔZ_{RVE}	0	0	0	0	0	0
LC10	0	0	0	0	0	0	ΔX_{RVE}	0	0
LC17	0	0	0	0	$\Delta Z_{RVE}/2$ $\Delta X_{RVE}/2$	0	ΔX_{RVE}	0	0

Table 4 Effective material parameters of shear MFC (FVF = 0.86) calculated with the EBHM (present) and AQBH (Trindade and Benjeddou 2011)

Material parameters	Constants	Unit	EBHM	AQBH	Difference ¹ /%
Shorted Young's moduli	\bar{Y}_1	GPa	26.63	26.72	0.34
	\bar{Y}_2	GPa	48.20	48.16	0.08
	\bar{Y}_3	GPa	23.47	23.63	0.68
Shorted shear moduli	\bar{G}_{23}	GPa	9.02	9.04	0.22
	\bar{G}_{13}	GPa	4.96	4.99	0.60
	\bar{G}_{12}	GPa	7.80	7.80	0.00
Shorted Poisson's ratios	$\bar{\nu}_{12}$	–	0.24	0.24	0.00
	$\bar{\nu}_{13}$	–	0.17	0.17	0.00
	$\bar{\nu}_{23}$	–	0.24	0.24	0.00
Piezoelectric strain constant	\bar{d}_{15}	pC/N	488.8	484.8	0.82
Piezoelectric stress constant	\bar{e}_{15}	C/m ²	2.43	2.20	9.94
Blocked dielectric constant	$\bar{\epsilon}_{11}^S$	nF/m	15.32	–	–
Free dielectric constant	$\bar{\epsilon}_{11}^T$	nF/m	16.51	14.85	10.59

¹ The relative difference is given by the absolute value of the difference between EBHM and AQBH related to the average of both. This refers also to Tables 5 and 6.

3.2 Results and discussion

To show the difference between the two evaluation schemes of AQBH (see section 2.2) and EBHM (see section 2.3) when dealing with piezoelectric modules with integrated electrodes, the evaluated effective material parameters (transformed to engineering constants in Voigt notation) are given in Table 4.

The effective mechanical material parameters comply with each other from both homogenization methods. The difference is low and may be caused by numerical inaccuracy. A relatively high difference can be noticed for the *stress* piezoelectric coupling coefficient \bar{e}_{15} and the *free* permittivity $\bar{\epsilon}_{11}^T$ which points out a difference between the two schemes for the evaluation of these parameters. In fact, on one hand, the primary output variables of the EBHM are the *e*-form \bar{e}_{15} and $\bar{\epsilon}_{11}^S$ constants (values in bold in Table 4, column EBHM), while the *d*-form constants \bar{d}_{15} and $\bar{\epsilon}_{11}^T$ are calculated a posteriori from these simplified single shear response mode's relations

$$\bar{d}_{15} = \frac{\bar{e}_{15}}{\bar{c}_{55}^E} \quad \bar{\epsilon}_{11}^T = \bar{\epsilon}_{11}^S + \frac{(\bar{e}_{15})^2}{\bar{c}_{55}^E} = \bar{\epsilon}_{11}^S + \bar{e}_{15}\bar{d}_{15} \quad (13a,b)$$

On the other hand, the primary output variables of the AQBH (see LC07 of Trindade and Benjeddou 2011) are the *d*-form \bar{d}_{15} and $\bar{\epsilon}_{11}^T$ constants (values in bold in Table 4, column AQBH), while the *e*-form constants \bar{e}_{15} and $\bar{\epsilon}_{11}^S$ have to be calculated a posteriori from above simplified single shear response mode's relations as follows (not done in Trindade and Benjeddou 2011)

$$\bar{e}_{15} = \bar{c}_{55}^E \bar{d}_{15} \quad \bar{\epsilon}_{11}^S = \bar{\epsilon}_{11}^T - \frac{(\bar{e}_{15})^2}{\bar{c}_{55}^E} = \bar{\epsilon}_{11}^T - \bar{e}_{15}\bar{d}_{15} \quad (14a,b)$$

After using Eqs. (13(a,b)) and (14(a,b)), the re-evaluated piezoelectric and dielectric constants are summarized in Table 5. The latter shows that there is now no significant difference between the stress piezoelectric constants from the two schemes. However, the dielectric constants are still different. This may be due to the different electromechanical boundary conditions used for their evaluations.

Table 5 Effective material parameters of shear MFC (FVF = 0.86) calculated with the EBHM (present) and AQBH (Trindade and Benjeddou 2011) *after using* Eqs. (13(a,b)) and (14(a,b))

Material parameters	Constants	Unit	EBHM	AQBH	Difference/%
Piezoelectric strain constant	\bar{d}_{15}	pC/N	489.92	484.80	1.05
Piezoelectric stress constant	\bar{e}_{15}	C/m ²	2.43	2.42	0.41
Blocked dielectric constant	$\bar{\epsilon}_{11}^S$	nF/m	15.32	13.68	11.31
Free dielectric constant	$\bar{\epsilon}_{11}^T$	nF/m	16.51	14.85	10.59

To investigate this influence of this persistent difference between the evaluated dielectric constants from the two schemes, the effective electromechanical coupling coefficient (EMCC) \bar{k}_{15} is estimated from the material parameters of Table 5 using the following definitions

$$\bar{k}_{15}^2 = \frac{\bar{e}_{15}^2}{\bar{c}_{55}^E \bar{\epsilon}_{11}^T} \qquad \bar{k}_{15}^2 = \frac{\bar{d}_{15}^2}{\bar{s}_{55}^E \bar{\epsilon}_{11}^T} \qquad (15a,b)$$

The results for the effective EMCC \bar{k}_{15} using these equations are shown in Table 6.

Table 6 Effective EMCC \bar{k}_{15} of shear piezoelectric MFC (FVF=0.86) calculated with EBHM (present) and AQBH (Trindade and Benjeddou 2011) *after using* Eqs. (13(a,b)) and (14(a,b)) and corresponding values from Table 5

EMCC, \bar{k}_{15}	EBHM	AQBH	Difference/ %
Eq. (15(a))	0.268	0.281	4.74
Eq. (15(b))	0.268	0.281	4.74

Both determination equations for the effective EMCC \bar{k}_{15} give the same results by each scheme; however, a reasonable relative difference of 4.74 % remains between the two schemes results. This can be attributed to the primary use of the *d*-form and *e*-form that require different electromechanical boundary conditions for the evaluation of the dielectric constants by AQBH and EBHM schemes, respectively. It can be then concluded that it is very important to use a single form of the constitutive equations for the RVE FE computations and to deduce *a posteriori* any other form constants by post-treatment.

4. Conclusions

The present work focused on presenting and validating, against open literature theoretical benchmarks, a new FE – based numerical homogenization procedure for the estimation of effective material parameters of composite piezoelectric modules with integrated electrodes. It evaluates the electromechanical enthalpy of the RVE FE model element-wise and estimates the effective material parameters from the summed electromechanical enthalpy. Therefore it gives the possibility of electric boundary conditions at the inner electrodes rather than at the RVE FE model boundaries. The approach was demonstrated with success on the theoretical concept of *transversely poled* shear piezoelectric MFC derived in (Trindade and Benjeddou 2011) and differences in the results were discussed. With this proposed new procedure a very strict and easy to program processing for homogenization of composite piezoelectric modules with integrated electrodes is available; this opens the possibility to incorporate them in comprehensive models and simulations of machinery and control systems.

The presently proposed EBHM was *applied* (Kranz *et al.* 2013) with success to characterize the *linear* piezoelectric constitutive parameters of a *realized* shear MFC but with piezoceramic fibers *polarized in their longitudinal direction*. Actuation testing of the *manufactured* MFC design (the main focus of the previously referenced work) has shown a nonlinear response with increasing actuation voltage. A first representation of this special nonlinearity has been handled by the AQBH (Trindade and Benjeddou 2013) by including the shear strain piezoelectric constant *nonlinear dependence on the actuation electric field* (the main focus of the previously referenced work).

As immediate perspectives and applications of the presently proposed EBHM, the resulting

effective electromechanical parameters, as evaluated in (Kranz *et al.* 2013), of the realized longitudinally poled shear MFC were used to simulate the latter's experimental sensing and blocking force responses. Corresponding experimental and preliminary simulation results are considered encouraging in the sense that they further validate this new homogenization procedure.

Acknowledgments

This research is supported by the German Research Foundation (Deutsche Forschungsgemeinschaft - DFG) in context of the Collaborative Research Centre/Transregio 39 PT-PIESA, subproject B2 and in context of the project "Investigation of the functional potential of piezo module integration into 3D structures" (DR 453/4-1).

The second author is supported by the Comet K2 Austrian Centre of Competence in Mechatronics (ACCM) at Linz, Austria.

References

- Benjeddou, A. and Al-Ajmi, M. (2011), "Analytical homogenizations of piezoceramic d_{15} shear macro-fibre composites", (Eds. Kuna, M. and Ricoeur, A.) , *IUTAM Symposium on Multiscale Modelling of Fatigue, Damage and Fracture in Smart Materials 2009*, volume 24 of *IUTAM Book series*, Springer, Netherlands.
- Berger, H., Kari, S., Gabbert, U., Rodriguez-Ramos, R., Bravo-Castillero, J., Guinovart-Diaz, R., Sabina, F.J. and Maugin, G.A. (2006), "Unit cell models of piezoelectric fiber composites for numerical and analytical calculation of effective properties", *Smart Mater. Struct.*, **15**(2), 451-458.
- Biscani, F., Nasser, H., Belouettar, S. and Carrera, E. (2011), "Equivalent electro-elastic properties of Macro-Fiber Composite (MFC) transducers using asymptotic expansion approach", *Compos. Part. B - Eng.*, **42**(3), 444-455.
- Deraemaeker, A. and Nasser, H. (2010), "Numerical evaluation of the equivalent properties of Macro Fiber Composite (MFC) transducers using periodic homogenization", *Int. J. Solids Struct.*, **47**(24), 3272-3285.
- Deraemaeker, A., Nasser, H., Benjeddou, A. and Preumont, A. (2009), "Mixing rules for the piezoelectric properties of macro fiber composites", *J. Intel. Mat. Syst. Str.*, **20**, 1475-1481.
- He, Q.C. (2004), "Variational and microstructure-independent relations for piezoelectric composites", *J. Mater. Sci. Technol.*, **20**, 69-72.
- Hori, M. and Nemat-Nasser, S. (1998), "Universal bounds for effective piezoelectric moduli", *Mech. Mater.*, **30**(1), 1-19.
- Kranz, B., Benjeddou, A. and Drossel W.G. (2013), "Numerical and experimental characterizations of longitudinally polarized piezoelectric d_{15} shear macro-fiber composites", *Acta Mech.*, DOI: 10.1007/s00707-013-0952-9.
- Malakooti, M.H. and Sodano, H.A. (2013), "Multi-inclusion modeling of multi-phase piezoelectric composites", *Compos. Pt. B*, **47**, 181-189.
- Paik, S.H., Yoon, T.H., Shin, S.J. and Kim, S.J. (2007), "Computational material characterization of active fiber composites", *J. Intel. Mat. Syst. Str.*, **18**, 19-28.
- Pettermann, H. E. and Suresh, S. (2000), "A comprehensive unit cell model: a study of coupled effects in piezoelectric 1-3 composites", *Int. J. Solids Struct.*, **37**, 5447-5464.
- Pindera, M.J., Khatam, H., Drago, A.S. and Bansal, Y. (2009), "Micromechanics of spatially uniform heterogeneous media: a critical review and emerging approaches", *Compos. Part. B - Eng.*, **40**(5), 349-378.
- Shindo, Y., Narita F., Sato, K. and Takeda, T. (2011), "Nonlinear electromechanical fields and localized polarization switching of piezoelectric macro-fiber composites", *J. Mech. Mater. Struct.*, **6** (7-8), 1089-

1102.

- Trindade, M.A. and Benjeddou, A. (2011), "Finite element homogenization technique for the characterization of d_{15} shear piezoelectric macro-fibre composites", *Smart Mater. Struct.*, **20**(7), 075012.
- Trindade, M.A. and Benjeddou, A. (2013), "Finite element characterization and parametric analysis of nonlinear behaviour of an actual d_{15} shear MFC", *Acta Mech.*, DOI: 10.1007/s00707-013-0951-x.
- Xu, Y., Zhang, W., Bassir, D. (2010), "Stress analysis of multi-phase and multi-layer plain weave composite structure using global/local approach", *Compos. Struct.*, **92**(5), 1143-1154.
- Zhang, W., Dai, G., Wang, F., Sun, S. and Bassir, H. (2007), "Using strain energy – based prediction of effective elastic properties in topology optimization of material microstructures", *Acta Mech. Sinica.*, **23**(1), 77-89.